

FREQUENCY COMPARISON (MASER 140 0805) - (BNM-SYRTE-FO2)
from MJD 53109 to MJD 53129 & MJD 53129 to MJD 53149

The primary frequency standard BNM-SYRTE-FO2 was compared to the hydrogen maser (1400805) of the laboratory, from MJD 53109 to MJD 53129 and then MMJD 53129 to MJD 53149.

The mean fractional frequency differences measured between the hydrogen Maser and fountain FO2 during the two periods are given in table I:

Period (MJD)	$Y(\text{Maser}) - Y(\text{FO2})$ (1)	u_B (2)	u_A (3)	$u_{\text{link / maser}}$ (4)
53109 – 53129	+6641,9	6,4	0,44	1,8
	+6645,4	6,2	0,45	2,2

Table I: Results of comparison in unity 1×10^{-16} .

Figure 1 collects the measurements of fractional frequency differences during the two periods. The measurements are connected for the systematic frequency shifts listed below.

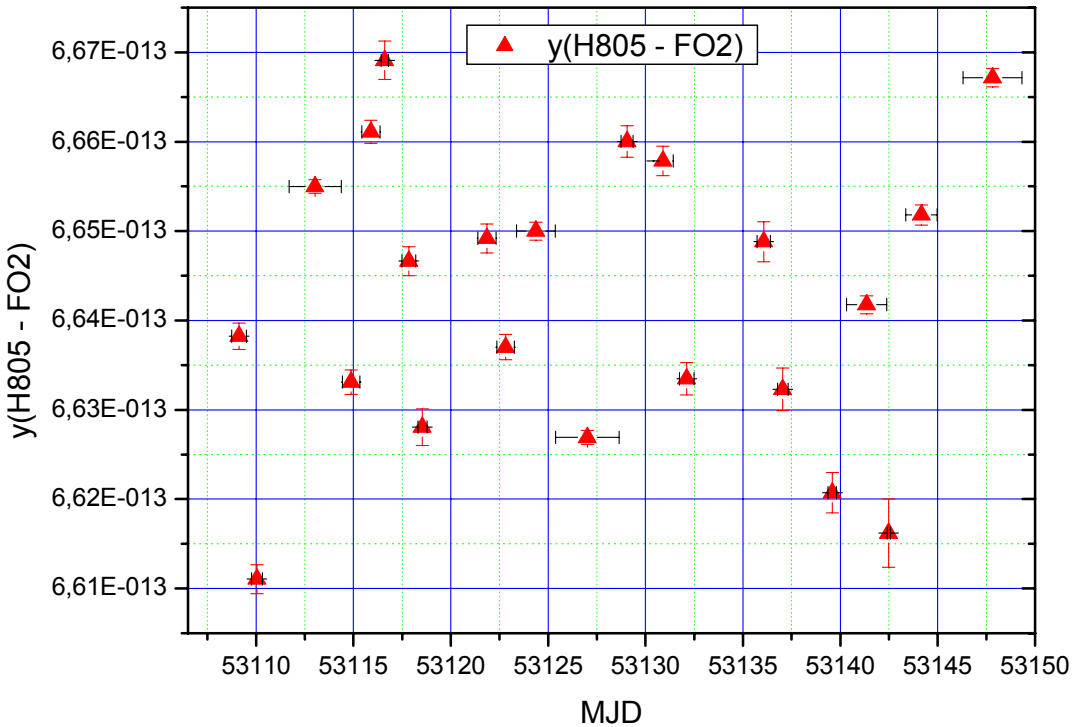


Figure 1: fractional frequency differences between Maser 1400805 & FO2 from MJD 53109 to MJD 53149

Table of measurements is given bellow (table 2).

FREQUENCY COMPARISON
 (MASER 1400805) - (BNM-SYRTE-FO2)
 FO2: Rubidium-Caesium Fontaine in Caesium mode

1st Period MJD 53108,75694 up to 53129,35833
 2nd Period MJD 53129,35833 au MJD 53149,33264

Start UTC dates unit MJD	Start Local dates unit H:M	Duration H :M	Mean fractional frequency difference $\gamma_{\text{Maser}} - \gamma_{\text{FO2}}$	type A uncertainties	
				σ_{Stat}	$\sigma_{\text{Collision}}$
53108,75694	13/04/2004 20:10	17:38	6,63823E-13	1,48E-16	2,84E-16
53109,77083	14/04/2004 20:30	13:30	6,61105E-13	1,63E-16	3,5E-16
53111,69792	16/04/2004 18:45	64:05	6,655E-13	7,45E-17	9,35E-17
53114,42847	19/04/2004 12:17	21:47	6,63309E-13	1,37E-16	3E-16
53115,43333	20/04/2004 12:24	22:18	6,6611E-13	1,3E-16	1,61E-16
53116,42014	21/04/2004 12:05	09:05	6,6691E-13	2,16E-16	2,77E-16
53117,48611	22/04/2004 13:40	17:19	6,64664E-13	1,62E-16	2,02E-16
53118,30556	23/04/2004 09:20	11:15	6,62806E-13	2,07E-16	2,8E-16
53121,38264	26/04/2004 11:11	22:37	6,64918E-13	1,63E-16	2,03E-16
53122,37083	27/04/2004 10:54	21:29	6,63702E-13	1,42E-16	1,77E-16
53123,37222	28/04/2004 10:56	47:35	6,65001E-13	1,01E-16	1,28E-16
53125,37986	30/04/2004 11:07	78:29	6,6269E-13	7,78E-17	9,96E-17
53128,73542	03/05/2004 19:39	14:57	6,66002E-13	1,78E-16	2,27E-16
53130,38056	05/05/2004 11:08	24:53	6,65784E-13	1,64E-16	1,99E-16
53131,73125	06/05/2004 19:33	18:10	6,63349E-13	1,8E-16	2,22E-16
53135,725	10/05/2004 19:24	16:28	6,64881E-13	2,24E-16	2,87E-16
53136,77569	11/05/2004 20:37	13:12	6,6323E-13	2,38E-16	3,05E-16
53139,36944	14/05/2004 10:52	10:29	6,62071E-13	2,26E-16	2,77E-16
53140,32153	15/05/2004 09:43	49:39	6,64175E-13	1,02E-16	1,24E-16
53142,39861	17/05/2004 11:34	04:10	6,6162E-13	3,81E-16	4,67E-16
53143,36458	18/05/2004 10:45	38:46	6,65181E-13	1,13E-16	1,43E-16
53146,31319	21/05/2004 09:31	72:28	6,66718E-13	1,03E-16	1,33E-16

Table 2: Measurements MaserH805 - FO2 from MJD 53109 to 53149

Start UTC dates unit MJD	Stop UTC dates unit MJD	Duration & Measurement Rate	Mean frequency difference normalized $\gamma_{\text{Maser}} - \gamma_{\text{FO2}}$ (1)	type A uncertainty $\sigma_{\text{Stat}} & \sigma_{\text{Collision}}$ (3)	Uncertainty due to the dead times σ_{deadTime} (4)
53108,75694	53129,35833	20,60139 j / 15,079167 j = 73,195 %	Standard Mean $\bar{\gamma} = 6643,5 \times 10^{-16}$ Weighted Mean (5): $\bar{\gamma} = 6644,6 \times 10^{-16}$ Linear fit regression (6): $\bar{\gamma} = 6645,2 \times 10^{-16}$	Linear fit regression $\sigma_A = 0,58 \times 10^{-16}$	$\sigma_{\text{deadTime}} = 1,5 \times 10^{-16}$
			Mean from Phase differences (7): $\bar{\gamma} = 6641,9 \times 10^{-16}$	From Phase differences $\sigma_A = 0,44 \times 10^{-16}$	
53130,38056	53149,33264	18,952 j / 10,34167 = 54,567 %	Standard Mean $\bar{\gamma} = 6641,1 \times 10^{-16}$ Weighted Mean (5): $\bar{\gamma} = 6648,8 \times 10^{-16}$ Linear fit regression (6): $\bar{\gamma} = 6646,7 \times 10^{-16}$	Linear fit regression $\sigma_A = 0,84 \times 10^{-16}$	$\sigma_{\text{deadTime}} = 1,9 \times 10^{-16}$
			Mean from Phase differences (7): $\bar{\gamma} = 6645,4 \times 10^{-16}$	From Phase differences $\sigma_A = 0,45 \times 10^{-16}$	

Table 3: Statistics of measurements

The different evaluations of the mean frequency over each period are close in order of magnitude of 1×10^{-16} .

SYRTE 61, avenue de l'Observatoire 75014 Paris - France tél 33 (0)1 40 51 22 04 fax 33 (0)1 40 51 22 91 e-mail direction.syrite@obspm.fr

Unité de recherche du CNRS 8630 site syrite.obspm.fr

- (1) Fractional frequency difference

$$y_{Maser} - y_{FO2} =$$

$$\text{Redshift} + \text{Zeeman2} + \text{BlackBody} + \text{Collision} + \text{CavityPulling} - \frac{f_{\text{measure}}}{f_0}$$

the relativistic effect is evaluated as: $\text{Redshift} = 0.654 \cdot 10^{-14}$ with an uncertainty $\sigma_{\text{Redshift}} = \pm 0.1 \cdot 10^{-15}$.

- (2) Systematic uncertainty $\sigma_B = u_B$ in which statistical effect of cold collisions and cavity pulling is removed (see annexe 1 & 2)

$$\sigma_B = \left(\sigma_{\text{Zeeman2}}^2 + \sigma_{\text{BlackBody}}^2 + \sigma_{\text{Collision Syst}}^2 + \sigma_{\text{Microwave Spectrum}}^2 + \sigma_{\text{Microwave Leakage}}^2 + \sigma_{\text{Ramsey Rabi}}^2 + \sigma_{\text{Recoil}}^2 + \sigma_{\text{second Doppler}}^2 + \sigma_{\text{Background collisions}}^2 + \sigma_{\text{Redshift}}^2 \right)^{(1/2)}$$

[ref. 1] - F. Pereira Dos Santos, H. Marion, M. Abgrall, S. Zhang, Y. Sortais, S. Bize, I. Maksimovic, D. Calonico, J. Grünert, C. Mandache, C. Vian, P. Rosenbuch, P. Lemonde, G. Santarelli, Ph. Laurent and A. Clairon BNM-SYRTE, C. Salomon, LKB, “Rb and Cs Laser Cooled Clocks: Testing the Stability of Fundamental Constants“, **Proceedings IEEE 2003, EFTF Tampa May 2003, p 55-67**

[ref. 2] - P. Wolf, BNMSYRTE, C.J. Bordé, LPL, “Recoil effects in microwave Ramsey spectroscopy”, arxiv: quant-ph/0403194

- (3) Statistical uncertainty $\sigma_A = u_A$, in which is taken into account the statistical uncertainty on each measurement σ_{Stat_i} and

statistical effect on the cold collisions and Cavity Pulling measurement $\sigma_{\text{Collision}_i}$ (see annexe 4 Linear Regression on the

frequency measurements & annexe 7): $\sigma_A = \sqrt{\frac{1}{\sum_{i=1}^n \frac{1}{\sigma_{\text{Stat}_i}^2 + \sigma_{\text{Collision}_i}^2}}}$

- (4) Uncertainty due to the link between maser and the fountain FO2 $u_{\text{link Maser}} = \sqrt{\sigma_{\text{link Lab}}^2 + \sigma_{\text{dead time}}^2}$ where $\sigma_{\text{link Lab}} = 0.1 \cdot 10^{-15}$ and $\sigma_{\text{dead time}}$ is the uncertainty due to the dead times during measurements (see annexe 3)

- (5) Weighted Mean by statistical uncertainty on each measurement

$$y_j := \frac{\sum_{i=1}^{n_j} \frac{y_i}{\sigma_{\text{Ai}}^2}}{\sum_{i=1}^{n_j} \frac{1}{\sigma_{\text{Ai}}^2}}$$

où

$$\sigma_{\text{Ai}} = \sqrt{\frac{1}{\sigma_{\text{Stat}_i}^2 + \sigma_{\text{Col}_i}^2}}$$

- (6) Mean frequency obtained by a linear fit by weighted least squares with statistical uncertainty on each measurement (see annexe 4).

- (7) Mean frequency obtained by phase differences, that is the retained result (see annexe 5)

ANNEXE 1

1 - Measurement of the collisional frequency shift and the cavity pulling

Collisional shift takes into account the effect of the collisions between cold Caesium atoms and the effect of "Cavity Pulling" whose influence also depends on the number of atom. This effect is measured in a differential way during each integration and its determination thus depends on the duration of the measurement and the stability of the clock, thus the uncertainty on the determination of the collisional shift is mainly of statistical nature. To the statistical uncertainty we add a type B uncertainty of 1% of frequency shift resulting from the imperfection of the adiabatic passage method (see the article "Controlling the Cold Collision Shift in High Precision Atomic Interferometry" of F. Pereira Back Santos, H. Marion, S. Bize, Y. Left, With. Bugle, and C. Solomon, Phys. Rev. Lett. 89, 233004 (2002)).

Figure 2 visualizes the relative frequency shift due to the effect of the collisions and "Cavity Pulling" of atomic fountain FO2 taken in low density, between the MJD 53109 and 53149 with the statistical uncertainty of each measurement.

Figure 3 shows the Allan deviation of a differential measurement using high and half atom density fountain configuration during MJD 53125, in order to correct of the cold collisional shift for this period. FO2 was operated alternatively (every 50 clock cycles) at low atomic density (red circle) and high density (black square) against the cryogenic oscillator weakly phase locked on the H maser. The measured density ratio between low and high densities is 0.5006 ± 0.0005 . The frequency difference between both densities is used to determine the collisional coefficient which is used to correct each data point. The blue triangle points represent the Allan deviation of the frequency difference between low and high densities when the points are corrected. The Allan deviation varies as $\tau^{-1/2}$ and reaches 10^{-16} after 3 days of integration.

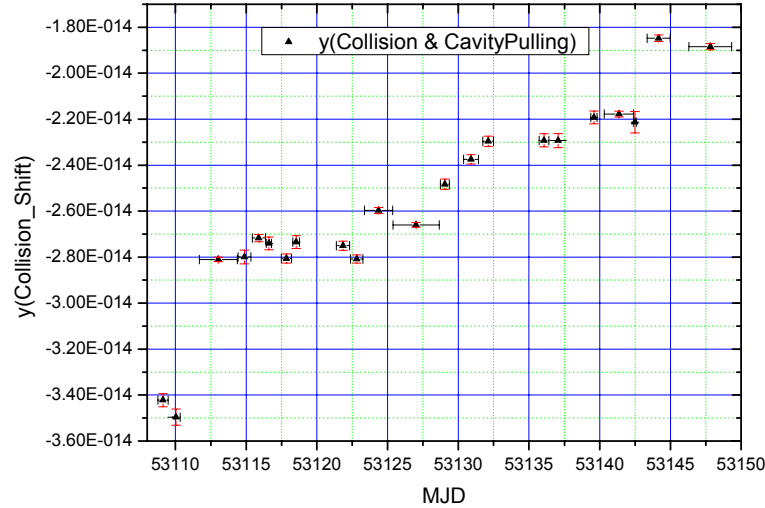


Figure 2: Fractional frequency shift due to cold collisions and Cavity Pulling from MJD 53109 to MJD 53149

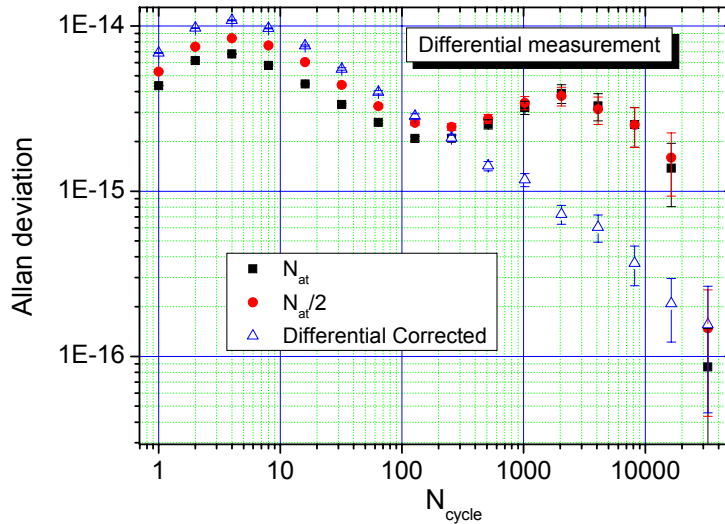


Figure 3: Allan deviation of measurements of the shift frequency in high and low atom density and their differences during MJD 53125

$$\sum_{i=1}^n \frac{y_{Collision_i}}{\sigma_{Collision_i}^2}$$

The weighted mean $y_{Collision_{moy}} = \frac{\sum_{i=1}^n \frac{y_{Collision_i}}{\sigma_{Collision_i}^2}}{\sum_{i=1}^n \frac{1}{\sigma_{Collision_i}^2}}$ of collisional shift gives for the whole period

$$y_{Collision_{moy}} := -0.2518 \cdot 10^{-13}$$

For April $y_{Collision_{moy_{avril}}} := -0.2750 \cdot 10^{-13}$ and for May $y_{Collision_{moy_{mai}}} := -0.2091 \cdot 10^{-13}$.

The systematic effect of these shifts is evaluated by the 1% part of the respective mean frequency collisional shift during April and May:

$$\sigma_{Collision_{Syst}} = \frac{1}{100} y_{Collision_{moy}} = \sigma_{Collision_{Syst}} := -0.2518 \cdot 10^{-15}$$

For April $\sigma_{Collision_{Syst_{avril}}} := -0.2750 \cdot 10^{-15}$

For May $\sigma_{Collision_{Syst_{mai}}} := -0.2091 \cdot 10^{-15}$

Those values are taking into account the systematic uncertainty evaluation σ_B (see annexe 2).

2 - Measurement of the 2nd order Zeeman frequency shift

Figure 4 displays the tracking of the central fringe of the field linearly dependant transition $|F=3; m_F=1\rangle \rightarrow |F=4; m_F=1\rangle$ measured every 15 min during MJD 53109 to MJD 53142. This shows the good stability of the magnetic field interrogated zone in an interval of $\pm 0.07\text{Hz}$. We conservatively take the peak to peak variation of the magnetic field over the whole measurement period as the field uncertainty of this effect which is thus equal to 20 pT. The corresponding uncertainty of the correction of the second order Zeeman effect is 0.4×10^{-16} .

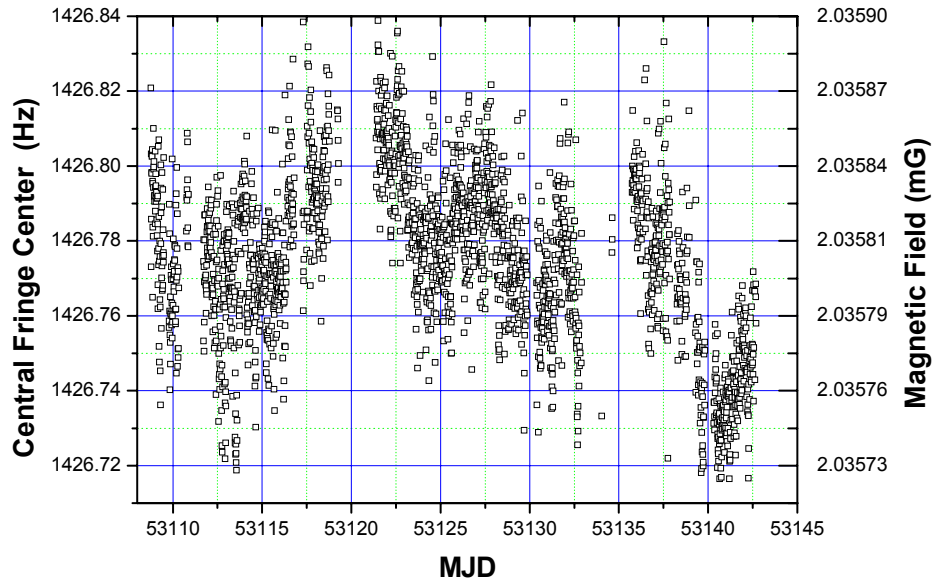


Figure 4: tracking of the central fringe from MJD 53109 to MJD 53142

ANNEXE 2

Uncertainties of systematic effects in the FO2 fountain

Systematic effects taken into account are the quadratic Zeeman, the Black Body, the cold collision and cavity pulling corresponding to the systematic part (see annexe 1), the microwave spectrum, the microwave leakage, the RamseyRabi pulling, the recoil, the 2nd Doppler, the background collisions. Each of these effects are affected by an uncertainty. The uncertainty of the red shift effect is also included in the systematic uncertainty budget and gives

$$\sigma_B = \left(\sigma_{Zeeman2}^2 + \sigma_{BlackBody}^2 + \sigma_{Collision_{Syst}}^2 + \sigma_{Microwave_Spectrum}^2 + \sigma_{Microwave_Leakage}^2 + \sigma_{Ramsey_Rabi}^2 + \sigma_{Recoil}^2 + \sigma_{second_Doppler}^2 + \sigma_{Background_collisions}^2 + \sigma_{Redshift}^2 \right)^{(1/2)}$$

Here are mentioned the uncertainties of the different effects (see [ref. 1]):

Zeeman effect	:	$\sigma_{Zeeman2} := 0.4 \cdot 10^{-16}$	(continuously measured see annexe 1)
Black Body effect	:	$\sigma_{BlackBody} := 0.46 \cdot 10^{-15}$	(calculated)
Systematic Collisional effect	:	$\sigma_{Collision_{Syst}} := -0.25 \cdot 10^{-15}$	(continuously measured)
Microwave Spectrum effect	:	$\sigma_{Microwave_Spectrum} := 0.20 \cdot 10^{-15}$	(calculated):
Microwave Leakage effect	:	$\sigma_{Microwave_Leakage} := 0.20 \cdot 10^{-15}$	(evaluated by changing microwave power)
Rabi-Ramsey effect	:	$\sigma_{Ramsey_Rabi} := 0.10 \cdot 10^{-15}$	(calculated)
Recoil effect (see [ref. 2])	:	$\sigma_{Recoil} < 0.10 \cdot 10^{-15}$	(calculated)
Second Doppler effect	:	$\sigma_{second_Doppler} := 0.8 \cdot 10^{-17}$	(calculated)
Background effect	:	$\sigma_{Background_collisions} := 0.10 \cdot 10^{-15}$	(evaluated)
Red shift effect	:	$\sigma_{Redshift} := 0.1 \cdot 10^{-15}$	(calculated)

For the whole period April Mai it gives

$$\Rightarrow \boxed{\sigma_B = 0.630 \cdot 10^{-15}}$$

For the period of April it gives:

$$\boxed{\sigma_{B_{April}} := 0.6395 \cdot 10^{-15}}$$

For the period of Mai it gives:

$$\boxed{\sigma_{B_{Mai}} := 0.6140 \cdot 10^{-15}}$$

ANNEXE 3

Uncertainty due to the dead time during the measurements

A statement of the distribution of the missed periods of measurements by FO2 is represented in figure 5.

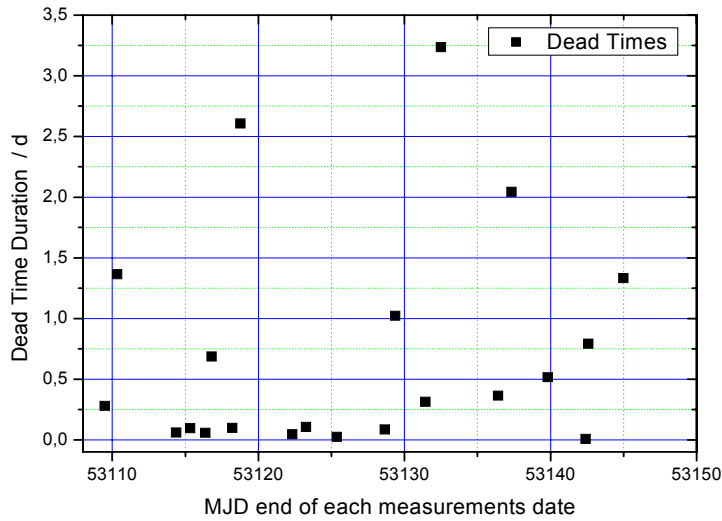


Figure 5 : Dead Times on measurements of MaserH805 –FO2 over the periode MJD 53109 up to 53149

For the period of the MJD 53109 until the MJD 53149, the variations of phase between hydrogen Maser 1400805 and the hydrogen Maser 1400816 were sampled every 100s. After removing a linear fit from the phase variations to carry out the calculation of standard deviation in the temporal field, we evaluated the uncertainty associated with the maser according to time (by step of 100s). One obtains the phase variations between Maser 1400805 and the Maser 1400816. They are on figure 6 (April) and 7 (May).

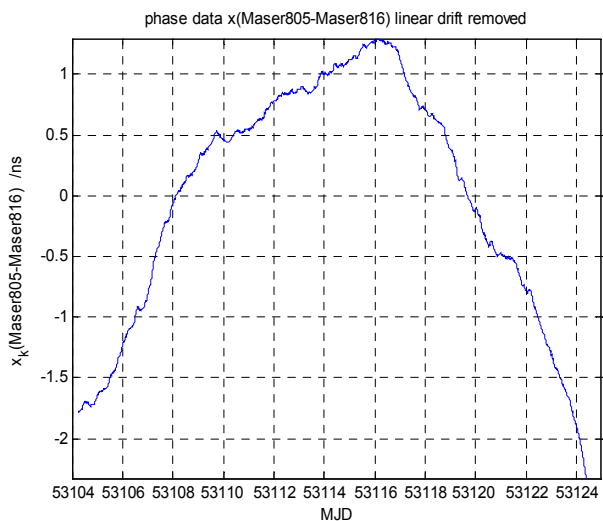


figure 6 : $x(H805-H816)$ MJD 53104 to MJD 53124 quadratic fit removed

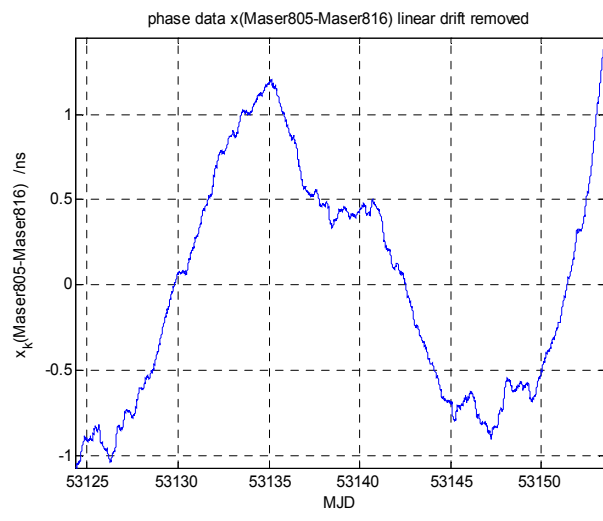


figure 7 : $x(H805-H816)$ MJD 53104 to MJD 53124 quadratic fit removed

Frequency stability analyzes were performed using the overlapping Allan deviation on frequency data and represented for April in figure 8 and for May in figure 9, and similarly time stability analyzes with a time deviation were computed and represented for April in figure 10 and for May in figure 11.

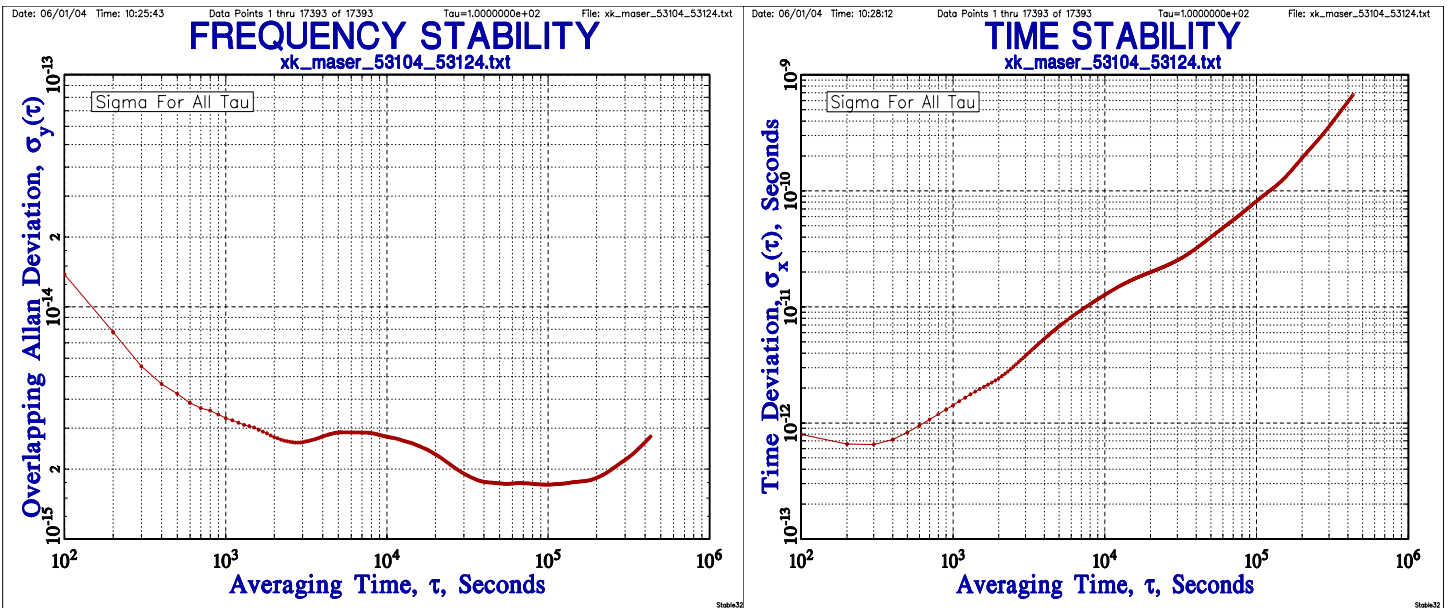


figure 8 : frequency stability analyzes x(HMaser805 - HMaser816) from MJD 53104 to MJD 53124

figure 10 : time stability analyzes from x(HMaser805 - HMaser816) from MJD 53104 to MJD 53124

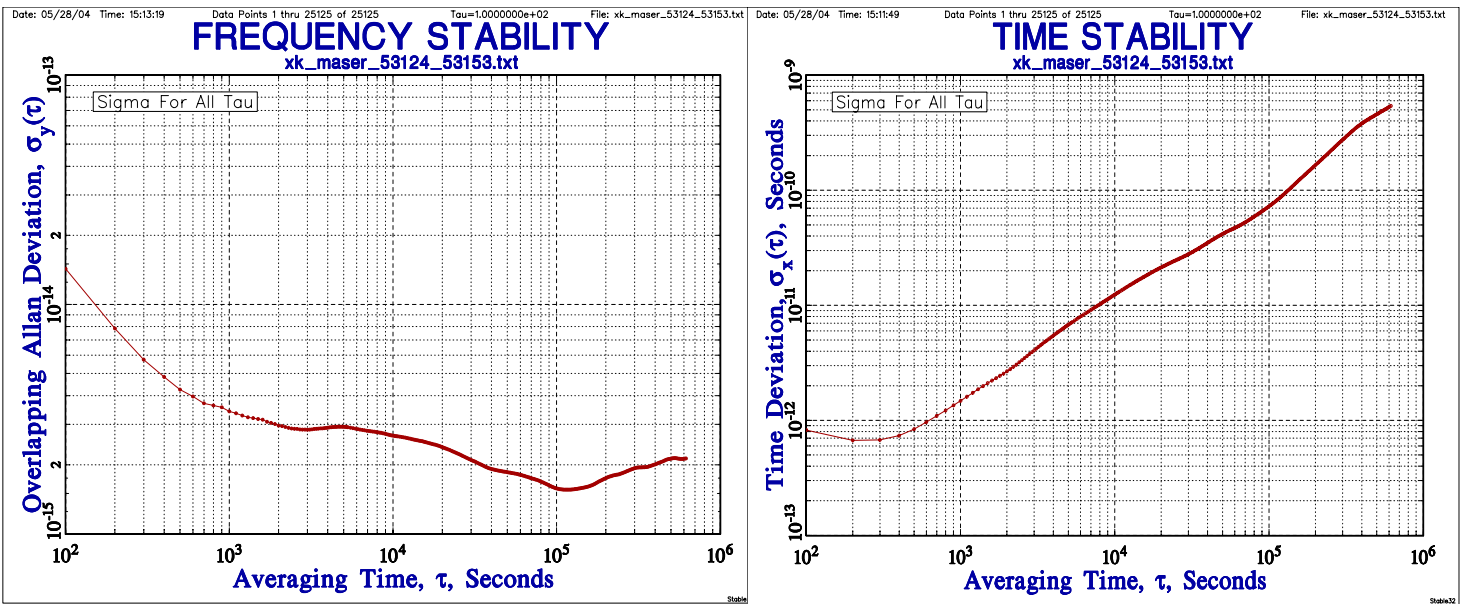


figure 9 : frequency stability analyzes from x(HMaser805 - HMaser816) from MJD 53124 to MJD 53153

figure 11 : time stability analyzes from x(HMaser805 - HMaser816) from MJD 53124 to MJD 53153

Tables 4 and 5 provide the standard deviations of the phase fluctuations of the hydrogen Maser 805 with respect to the hydrogen Maser 816 associated to each dead time according to their duration for the respective periods April and May. The quadratic sum gives

$$\sum_{i=1}^{12} \sigma_x(\tau)_i^2 = 0.672 \cdot 10^{-19}$$

During the April period of FO2 measurements 20,6 days $T = 0.1779960096 \cdot 10^7$ seconds. One thus finds the standard deviation of the fluctuations of frequency due to the dead times in measurements by the ratio

$$\sqrt{\frac{\sum_{i=1}^{12} \sigma_x(\tau)_i^2}{T}} = 0.1456 \cdot 10^{-15}$$

$$\sigma_{deadTime} := 0.1456 \cdot 10^{-15} \text{ and so } \sigma_{link_Maser} = \sqrt{\sigma_{link_lab}^2 + \sigma_{deadTime}^2} \text{ that gives}$$

$$\sigma_{link_Maser} = 0.177 \cdot 10^{-15}$$

End Date of each measurement (MJD)	Dead Time Duration HH : M second		σ_x
53109,49167	06:42	24119,99997	2.2126e-11
53110,33333	32:45	117900,00001	9.6158e-11
53114,36806	01:27	5220,00001	7.0883e-12
53115,33611	02:20	8399,99998	1.1125e-11
53116,3625	01:23	4979,99998	6.8083e-12
53116,79861	16:30	59400	4.7872e-11
53118,20764	02:21	8460,00002	1.1125e-11
53118,77431	62:36	225360,00001	2.3358e-10
53122,325	01:06	3960,00001	5.3292e-12
53123,26597	02:33	9179,99998	1.1992e-11
53125,35486	00:36	2159,99999	2.6602e-12
53128,65	06:42	7380	9.7631e-12
53129,35833	-	-	--

Table 4 : Statement of the dead times of Maser 805 - FO2 measurements between MJD 53119 and MJD 53129

During May, from MJD 53125 to MJD 53153 we used the phase differences between HMaser805 – HMaser816 sampled by periodical interval of 100s. In figure 7 are plotted the phase differences linear fit removed. The Allan deviation in frequency domain is plotted in figure 8 and in time domain in figure 9. Table 5 report the time deviation corresponding to the dead time duration for this period.

End Date of each measurement (MJD)	Dead Time Duration HH : M second		σ_x
53131,41736	07:32	27119,99999	2.6197e-11
53132,48819	77:41	279659,99999	2.5245e-10
53136,41111	08:45	31500,00001	2.8904e-11
53137,32569	49:03	176580,00002	1.4341e-10
53139,80625	12:22	44520	3.8197e-11
53142,39028	00:12	720	1.0937e-12
53142,57222	19:01	68459,99998	5.1738e-11
53144,97986	32:00	115200,00001	8.3900e-11
53149,33264	--	--	--

Tableau 5 : Statement of the dead times of Maser 805 - FO2 measurements between MJD 53129 and MJD 53149

Over the May period of FO2 measurements 18,95 days $T := 0.163745971200024 \cdot 10^7$ seconds. One thus finds the standard deviation of the fluctuations of frequency due to the dead times in measurements by the report/ratio

$$\frac{\sqrt{\sum_{i=1}^{12} \sigma_x(\tau_i)^2}}{T} = 0.1902 \cdot 10^{-15}$$

$$\sigma_{deadTime} := 0.1902 \cdot 10^{-15} \text{ and so } \sigma_{link_Maser} = \sqrt{\sigma_{link_lab}^2 + \sigma_{deadTime}^2} \text{ that gives } \boxed{\sigma_{link_Maser} = 0.215 \cdot 10^{-15}}$$

Linear Regression on the frequency measurements on period MJD 53109-53129

One calculates the linear regression line by the algorithm of weighted least squares by statistical uncertainty of each frequency differences measurements.

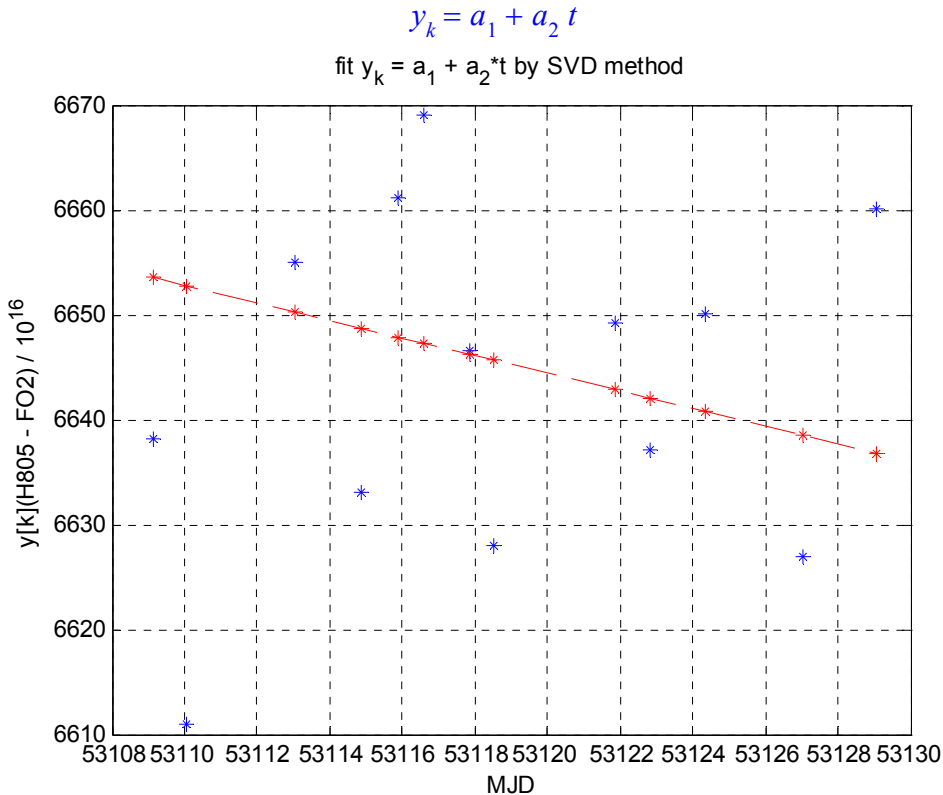


Figure 12: linear regression on the frequency y (Maser-FO2) between MJD 53109 and 53129 weighted by uncertainty : $1 / \sigma_{A_i}^2$

Covariance Matrix:

$$\begin{matrix} 2.56739017990266e-025 & -4.83321400325803e-030 \\ -4.83321400325803e-030 & 9.09871748005562e-035 \end{matrix}$$

Mean date of measurement = 53119.085595

Frequency mean by linear fit $y_{FO2} = 6.64518557316399e-013$

Uncertainty propagation at t_{moyen} $uc_{y_{FO2}} = 5.83827140183209e-017$

Degree of Freedom DEF = 11

Chi2/DEF = 43.2005898839323

Birge ratio $R_b = (\chi^2/\text{DEF})^{1/2} = 6.57271556389992$

Limit of Birge ratio $R_b = 1 + \sqrt{2/\text{DEF}} = 1.42640143271122$

Probability of a sample y (Maser-FO2) being superior of $\chi^2|\text{DEF}$ = 3.031593576634792e-095

SSR = Sum Square of Residues: 4.02755207969501e-029

RMS Residues: 6.34629977206798e-015

Allan Variance = 3.017624041666700e-030

Allan Deviation = 1.737130979997392e-015

Allan Deviation at T with assumption of White Frequency Noise = 4.642677830786498e-016

T (seconds) = 1916880.10338494

Linear Regression on the frequency measurements on period MJD 53129-53149

One calculates the linear regression line by the algorithm of weighted least squares by statistical uncertainty of each frequency differences measurements.

$$y_k = a_1 + a_2 t$$

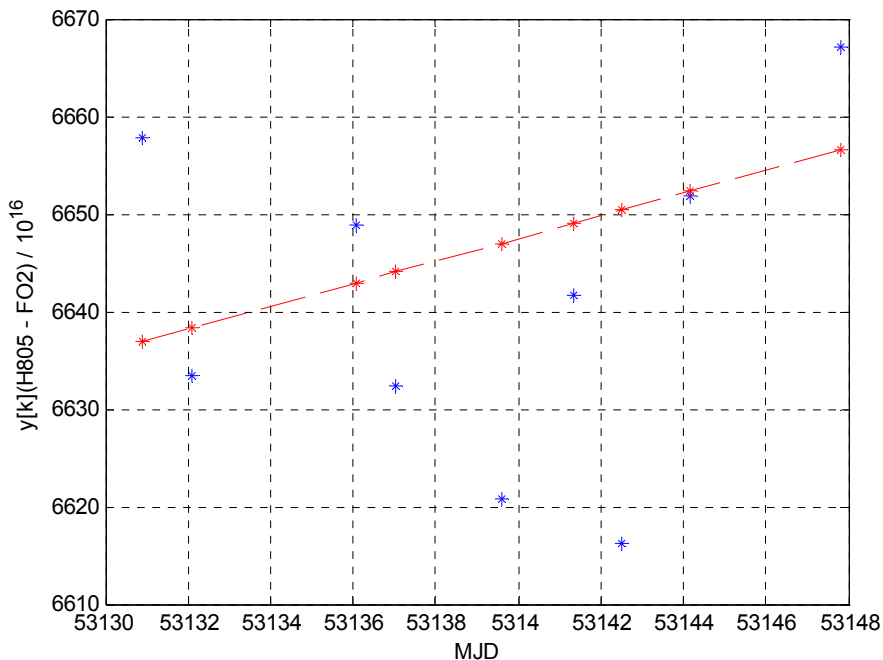


Figure 13: linear regression on the frequency y (Maser-FO2) between MJD 53129 and 53149 weighted by uncertainty : $1 / \sigma_{A_i}^2$

Covariance Matrix:

$$\begin{matrix} 5.93029491953144e-025 & -1.1159521289945e-029 \\ -1.1159521289945e-029 & 2.09997847415645e-034 \end{matrix}$$

Mean date of measurement = 53139.36094

Frequency mean by linear fit $y_{FO2} = 6.64672657366523e-013$

Uncertainty propagation at t_{moyen} $uc_{y_{FO2}} = 8.39570317588391e-017$

Degree of Freedom DEF = 7

Chi2/DEF = 32.4853154607255

Birge ratio $R_b = (\text{chi2}/\text{DEF})^{1/2} : 5.69958906068898$

Limit of Birge ratio $R_b = 1 + \sqrt{2/\text{DEF}} = 1.53452248382485$

Probability of a sample y (Maser-FO2) being superior of $\text{Chi2}|\text{DEF} = 8.671720306051134e-046$

SSR = Sum Square of Residues: 2.65788820609706e-029

RMS Residues: 5.1554710804126e-015

Allan Variance = 2.396453875000017e-030

Allan Deviation = 1.548048408480826e-015

Allan Deviation at T with assumption of White Frequency Noise = 4.293513779752339e-016

T (seconds) = 1773914.68800026

Mean Frequency computed by phase differences

On figure 14 is represented the evolution of the differences in fractional frequency $y(t)$. At each period of integration is evaluated a frequency \bar{y}_k corresponding to the interval $t_{k+1} - t_k$. The relation binding the variations of phase and the instantaneous frequency deviations is given by

$$y_k = \frac{x_{k+1} - x_k}{t_{k+1} - t_k} \quad (1)$$

$$y(t) = \frac{\nu_{H\text{Maser}} - \nu_{FO2}}{\nu_0}$$

$$\nu_0 = 9,192631770 \text{ GHz}$$

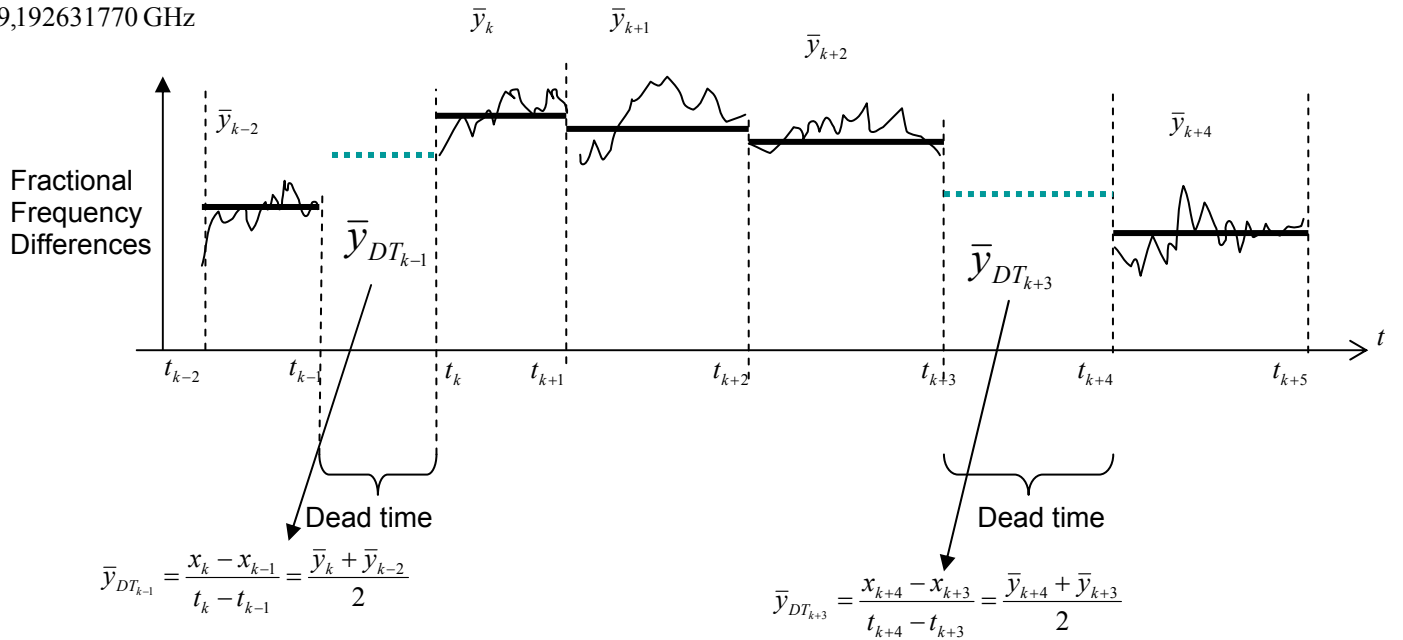


figure 14 : contribution of frequency measurements on the mean frequency calculated

by using equation (1) we have $x_{k+1} - x_k = (t_{k+1} - t_k) y_k$

and for addition of consecutive phase differences we find $\sum_{k=1}^N (x_{k+1} - x_k) = x_{N+1} - x_1 = \sum_{k=1}^N (t_{k+1} - t_k) y_k$

During dead time we evaluated the mean frequency by interpolating the mean frequency between two intervals of integrations noted :

$$y_{DT_{m-1}} = \frac{1}{2} y_m + \frac{1}{2} y_{m-1} \quad (2)$$

The contribution of N duty intervals with the frequency measurements y_k and M idle intervals with the mean frequency extrapolating between two intervals of integration y_{DT} give the summation

$$\left(\sum_{k=1}^N (t_{k+1} - t_k) y_k \right) + \left(\sum_{m=1}^M (t_{m+1} - t_m) y_{DT_m} \right) = x_{fin} - x_{deb} \quad (3)$$

$$y_{moy} = \frac{x_{fin} - x_{deb}}{86400 \text{ MJD}_{fin} - 86400 \text{ MJD}_{deb}}$$

where $x_{fin} - x_{deb}$ represent the phase variation between the whole periods of integration.

The evaluation of statistical uncertainty on each phase differences data extracted from fractional frequency differences, is given as we have in presence of white frequency noise in each period of measurement, by the expression

$$\sigma_x(\tau_i)^2 = \sigma_y(\tau_i)^2 \tau_i^2$$

For the whole period T of measurement that gives in frequency instability

$$\sigma_y(\tau) = \sqrt{\frac{\sum_{i=1}^N \sigma_y(\tau_i)^2 \tau_i^2}{T}}$$

with N = 13 in April and $T = 0.1779960096 \cdot 10^7$ seconds it gives

$$\sigma_y(\tau) = \sqrt{\frac{\sum_{i=1}^{13} \sigma_y(\tau_i)^2 \tau_i^2}{T}} = 0.439 \cdot 10^{-16}$$

$$\boxed{\sigma_A = 0.439 \cdot 10^{-16}}$$

with N = 9 in Mai and $T := 0.163745971200024 \cdot 10^7$ seconds it gives

$$\sigma_y(\tau) = \sqrt{\frac{\sum_{i=1}^9 \sigma_y(\tau_i)^2 \tau_i^2}{T}} = 0.446 \cdot 10^{-16}$$

$$\boxed{\sigma_A = 0.446 \cdot 10^{-16}}$$

The evaluation of the mean frequency between two intervals of integrations during the period from MJD 53109 to MJD 53129 is given. Figure 15 gives the frequency differences between HMaser 805 and FO2 (blue plus) and the mean frequency during dead times (magenta stars):

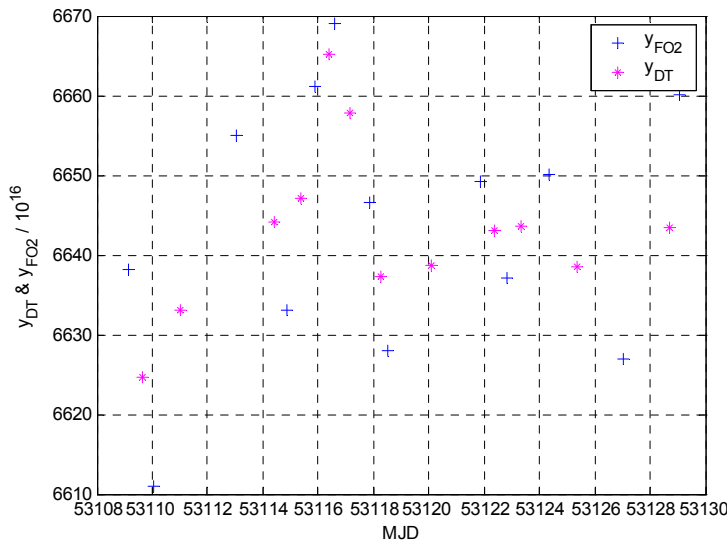


figure 15 : frequency differences HMaser805 and FO2 from MJD 53109 up to MJD 53129

From equation (3) we find the phase difference over the whole period of integration

$$x_{fin} - x_{deb} = 1.18223 \text{ } \mu\text{s}$$

This value is replaced in equation (4) above for computation of y_{moy} during this period. We find

$$\boxed{y_{moy} = 0.66419 \cdot 10^{-12}}$$

The evaluation of the mean frequency between two intervals of integrations during the period MJD 53129 to MJD 53149 is given. Figure 16 gives the frequency differences between HMaser 805 and FO2 and the mean frequency FO2 (blue plus) and the mean frequency during dead times (magenta stars):

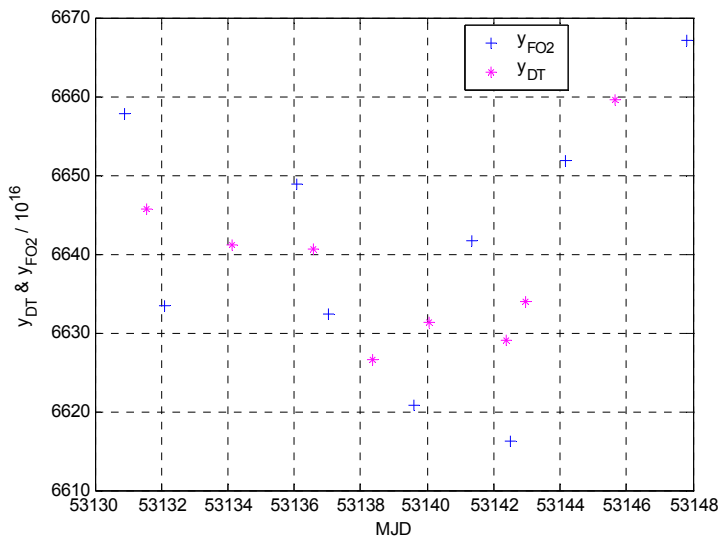


figure 16 : frequency differences HMaser805 and FO2 from MJD 53129 up to MJD 53149

From equation (3) we find the phase difference over the whole period of integration

$$x_{fin} - x_{deb} = 1.08816 \text{ } \mu\text{s}$$

This value is replaced in equation (4) above for computation of y_{moy} during this period. We find

$$y_{moy} = 0.66454 \cdot 10^{-12}$$